EPJ Web of Conferences will be set by the publisher
DOI: will be set by the publisher

First 13 TeV results from CMS

Ferenc Siklér[1,a] for the CMS Collaboration

[1] *Wigner RCP, Budapest, Hungary*

Abstract. An overview of the first 13 TeV results from CMS is presented, including measurements of pseudorapidity-density of charged hadrons, two-particle angular correlations, inclusive $t\bar{t}$ and single top production, as well as exotica.

1 Pseudorapidity-density of charged hadrons

The pseudorapidity-density of charged hadrons ($dN_{ch}/d\eta$) is one of the most basic physical observables in high-energy particle collisions. It presents the essential first step in exploring the physics of a new energy regime, since it reflects the combination of perturbative and nonperturbative QCD effects: saturation of parton densities, multiparton interactions, parton hadronization, and soft diffractive scattering. In CMS the measurement was performed under special circumstances. Because of a cryogenic problem, no magnetic field could be maintained during the first stable collisions. Hence it was impossible to measure particle charge or momentum, but only direction.

Inelastic collision events were selected online, where a coincidence of signals from both beam-sensing devices was required, indicating the presence of both proton bunches crossing the interaction point; and offline, where at least one reconstructed interaction vertex is needed, according to the tracklet or track vertex reconstruction methods described below. While only the reconstructed collision vertex with the highest multiplicity is used in the tracklet analysis, all reconstructed vertices in a given bunch crossing are processed for the track analysis.

The results are corrected to correspond to a sample of inelastic collisions [1]. The corrections from the detector-level offline event selection to the hadron-level event definitions are derived from MC simulations with Pythia8 v208 [2, 3] (several tunes [4]) and Epos LHC [5] (LHC tune [6]), which cover a wide range of possible model ingredients. The detector response is simulated with Geant4 [7] and processed through the same event reconstruction chain as collision data. The MC simulations are produced with the location and shape of the interaction region as extracted from data.

The analysis of the recorded data is performed with two reconstruction techniques based on hits of charged particles detected by the CMS pixel detector. (A very preliminary result from June, using hits only from the strip tracker, is displayed in Fig. 1-left.) While both start by searching for hit pairs in different layers at similar azimuthal angles ϕ (Fig. 1-right), the tracklet method (using hit pairs) performs background subtraction based on control samples in data, while the track method (using hit triplets) minimizes background contributions by requiring an additional hit in the detector. This results in a slightly narrower accessible η range for the track method as compared to the tracklet method.

[a] e-mail: sikler.ferenc@wigner.mta.hu

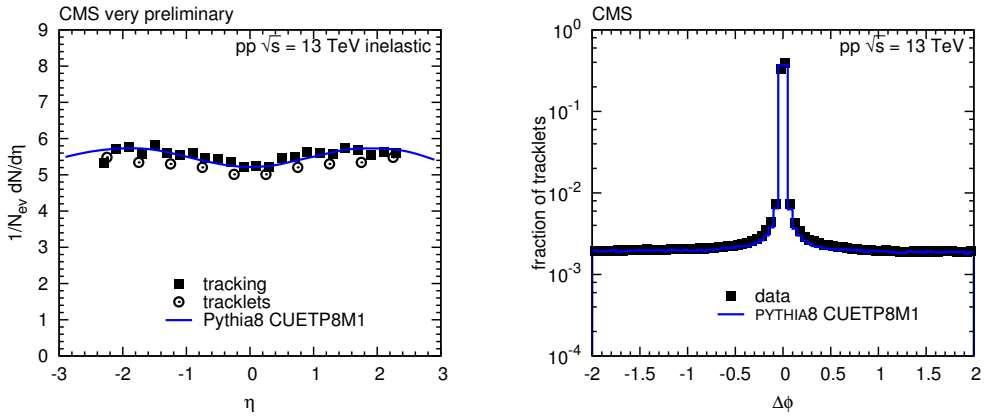

Figure 1. Left: Distributions of the pseudorapidity density of charged hadrons in inelastic pp collisions at 13 TeV measured in *strip-only data* (solid markers, tracking and tracklet results), and predicted by the PYTHIA8 CUETP8M1 event generator (curve) [8]. Right: The $\Delta\phi$ distributions of hit pairs on tracklets in the pixel data (squares) and from MC simulation (histogram) [1].

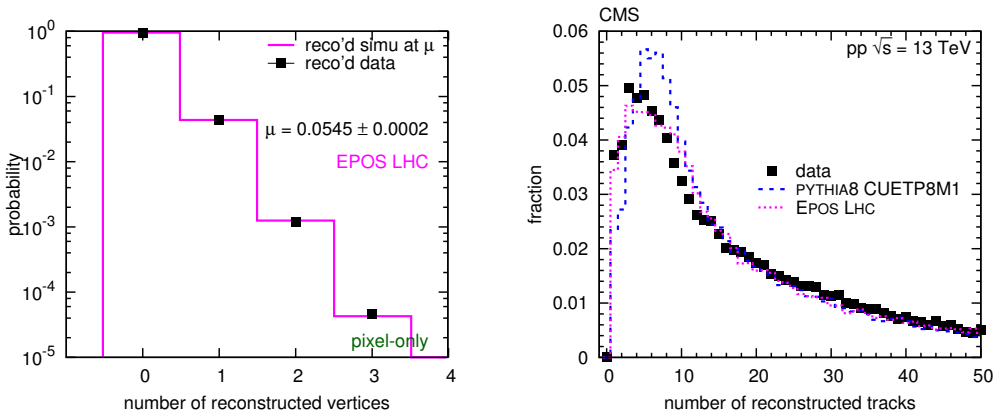

Figure 2. Left: Distribution of the number of reconstructed vertices from data and that based on the EPOS LHC model including simulations. The extracted mean (μ) of the corresponding Poissonian is also indicated. Right: Distributions of the number of reconstructed tracks per event from data and from simulations, for inelastic pp collisions [1].

Since various factors, such as detector alignment, material, detector response, and dependence on MC event generators, influence the two techniques somewhat differently, their final combination into a single measurement provides a more robust result.

For the tracklet analysis, all recorded bunch crossings are processed (about 170 000 collision events), while for the track analysis only 1 million of them are used (about 55 000 collision events). After corrections, the agreement between the tracklet and track $\mathrm{d}N_{\mathrm{ch}}/\mathrm{d}\eta$ results is better than 2% at

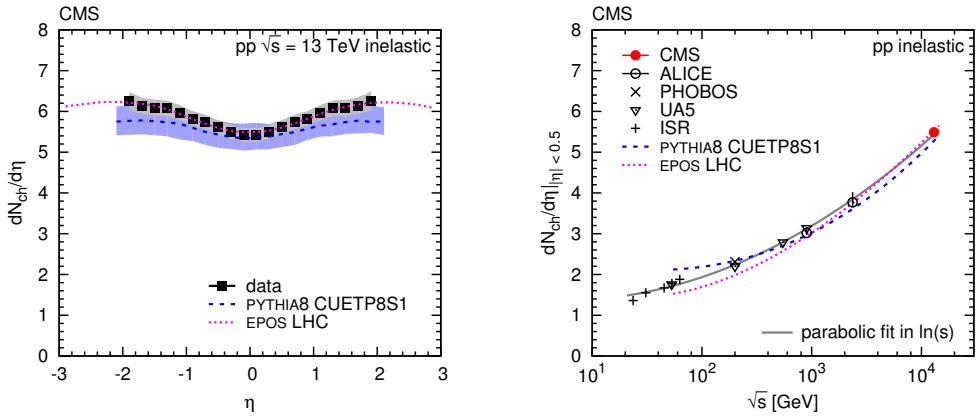

Figure 3. Left: Distributions of the pseudorapidity density of charged hadrons in the region $|\eta| < 2$ in inelastic pp collisions at 13 TeV measured in data (solid markers, combined track and tracklet results, symmetrized in η), and predicted by the Pythia8 CUETP8S1 and the Epos LHC event generators (curves) [1]. The grey shaded area encompassing the data points indicates their correlated systematic uncertainties. The blue band corresponds to the envelope of the CUETP8S1 tune parametric uncertainties. Right: Center-of-mass energy dependence of $\mathrm{d}N_{\mathrm{ch}}/\mathrm{d}\eta|_{|\eta|<0.5}$ including lower energy data [1]. The solid curve shows a second-order polynomial in $\ln(s)$ fit to the data points, including the new result at $\sqrt{s} = 13$ TeV. The dashed and dotted curves show the Pythia8 CUETP8S1 and Epos LHC predictions, respectively.

central pseudorapidity and better than 3% at forward pseudorapidities. Hence, averaging their $\mathrm{d}N_{\mathrm{ch}}/\mathrm{d}\eta$ values is justified. Since the systematic uncertainties dominate and are mostly correlated between the two analyses, the simple mean of the central values and of systematic uncertainties are taken. The fraction of primary charged leptons is about 1% of the total long-lived charged particles produced, and the correction from detector-level tracklets and tracks is done for charged hadrons only.

The performance of vertexing in simulation and in data was compared and used to estimate the average inelastic interaction probability μ per bunch crossing by assuming a Poissonian distribution (Fig. 2-left). While Pythia8 CUETP8M1 gives $\mu = 0.0525 \pm 0.0003$, Epos LHC leads to 0.0545 ± 0.0002. The product of the number of analyzed bunch crossings and μ gives the number of inelastic collision events, to be used for the calculation of the final $\mathrm{d}N_{\mathrm{ch}}/\mathrm{d}\eta$ values. As Fig. 2-right shows, the distribution of the number of reconstructed tracks in data is in fair agreement with the MC event generator predictions in particular at the higher multiplicities.

Pseudorapidity density distributions of charged hadrons in the region $|\eta| < 2$ for inelastic pp events are shown in Fig. 3-left. The data points and uncertainties are symmetrized in $\pm\eta$. While the predictions of both Pythia8 (with CUETP8S1 and CUETP8M1) and Epos LHC agree with the measured central value, the measured $\mathrm{d}N_{\mathrm{ch}}/\mathrm{d}\eta$ distribution in the full η range is better described by the latter. The uncertainty band of Pythia8 corresponds to the envelope of the uncertainties of the tune parameters of CUETP8S1; the Epos LHC predictions have no uncertainty associated with its parameter settings.

For central pseudorapidities ($|\eta| < 0.5$), the charged-hadron multiplicity density is $\mathrm{d}N_{\mathrm{ch}}/\mathrm{d}\eta|_{|\eta|<0.5} = 5.49 \pm 0.01(\mathrm{stat}) \pm 0.17(\mathrm{syst})$, a value obtained by combining the two methods.

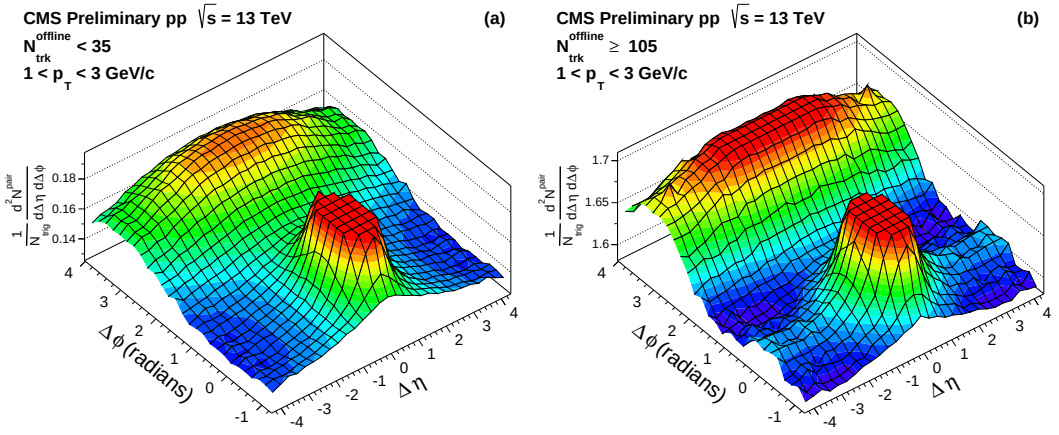

Figure 4. The 2D $(\Delta\eta, \Delta\phi)$ two-particle correlation functions in pp collisions at $\sqrt{s} = 13$ TeV for pairs of charged particles both in the range $1 < p_{\mathrm{T}} < 3$ GeV/c. Results are shown for (a) low-multiplicity events $N_{\mathrm{track}}^{\mathrm{offline}} < 35$) and for (b) a high-multiplicity sample ($N_{\mathrm{track}}^{\mathrm{offline}} \geq 105$). The sharp peaks from jet correlations around $(\Delta\eta, \Delta\phi) = (0, 0)$ are truncated to better illustrate the long-range correlations.

The center-of-mass energy dependence of $\mathrm{d}N_{\mathrm{ch}}/\mathrm{d}\eta$ is shown in Fig. 3-right. For comparison, inelastic pp measurements at lower energies (ISR [9, 10], UA5 [11, 12], PHOBOS [13], and ALICE [14]) are also plotted. The measured values are empirically fitted using a second-order polynomial in $\ln(s)$ as $1.55 - 0.113\ln(s) + 0.0168\ln(s)^2$ which provides a good description of the available data over the full energy range. The Pythia8 and Epos LHC event generators globally reproduce the collision-energy dependence of hadron production in inelastic pp collisions.

These results constitute the first CMS measurement of hadron production at the new center-of-mass energy frontier, and provide new constraints for the improvement of perturbative and nonperturbative QCD aspects implemented in hadronic event generators.

2 Angular correlation of charged hadrons

CMS has performed studies of two-particle angular correlations for charged particles produced in pp collisions at a center-of-mass energy of 13 TeV [15], with a special emphasis on the long-range near-side two-particle structure seen in lower energy pp and pPb collisions. The data correspond to an integrated luminosity of about 270 nb^{-1}.

The correlations are studied over a broad range of pseudorapidity ($|\eta| < 2.4$) and over the full azimuth (ϕ) as a function of charged particle multiplicity and transverse momentum. In high-multiplicity events, a long-range ($|\Delta\eta| > 2.0$), near-side ($\Delta\phi \approx 0$) structure emerges in the two-particle $\Delta\eta - \Delta\phi$ correlation functions (Fig. 4). The magnitude of the correlation exhibits a pronounced maximum in the range $1.0 < p_{\mathrm{T}} < 2.0$ GeV/c and an approximately linear increase with the charged particle multiplicity (Fig. 5). The overall correlation strength at $\sqrt{s} = 13$ TeV is similar to that found in earlier pp data at $\sqrt{s} = 7$ TeV, but is measured up to much higher multiplicity values.

The near-side long-range yield obtained with the zero-yield-at-minimum (ZYAM) procedure is found to be consistent with zero in the low-multiplicity region, with an approximately linear increase

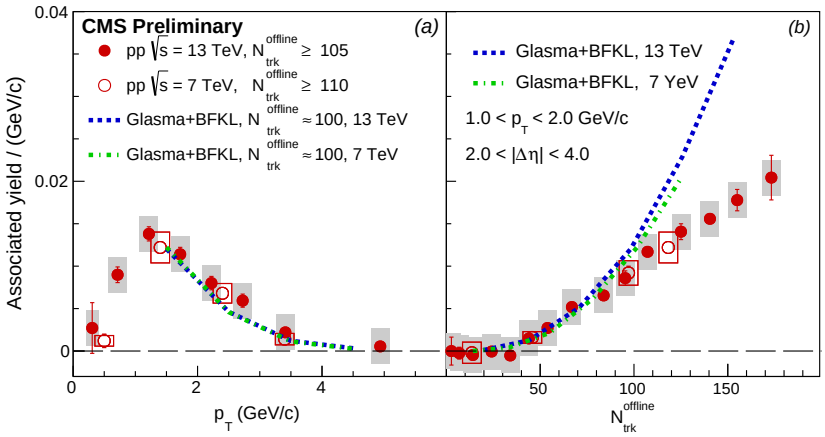

Figure 5. Associated yield for the near side of the correlation function averaged over $2 < |\Delta\eta| < 4$ and integrated over the region $|\Delta\phi| < \Delta\phi_{\mathrm{ZYAM}}$ for pp data at $\sqrt{s} = 13\,\mathrm{TeV}$ (filled circles) and 7 TeV (open circles). Panel (a) shows the associated yield as a function of p_{T} for $N_{\mathrm{track}}^{\mathrm{offline}} \geq 105$. In panel (b) the associated yield for $1 < p_{\mathrm{T}} < 2$ GeV/c is shown as a function of multiplicity $N_{\mathrm{track}}^{\mathrm{offline}}$. The p_{T} selection applies to both particles in each pair. The error bars correspond to the statistical uncertainties, while the shaded areas and boxes denote the systematic uncertainties. Curves represent calculations from the gluon saturation model [16].

with multiplicity $N_{\mathrm{trk}}^{\mathrm{offline}} \gtrsim 40$. A strong collision system size dependence is observed when comparing data from pp, pPb, and PbPb collisions. Comparing the pp data at $\sqrt{s} = 7\,\mathrm{TeV}$ and 13 TeV, no collision energy dependence of the near-side associated yields is observed over the overlapping event multiplicity and p_{T} ranges.

3 Top production

The study top production has a great discovery potential for physics beyond the standard model. It helps to test the production mechanisms, to check the validity of QCD, and to provide an important source of background in searches for physics beyond the standard model.

Top quarks can decay leptonically $\mathrm{t} \to \mathrm{W\,b} \to (\mathrm{l}\,\nu)$ (b-jet), and hadronically $\mathrm{t} \to$ hadrons (three jets). In case of top pair production, di-leptonic decays of both quarks can be selected by requiring one electron and one muon of opposite charge, and at least two jets in the final state. The case when one decay is leptonic and the other one is hadronic is selected by asking for one electron or one muon, and at least four jets in the final state. The measurements detailed below all use data corresponding to an integrated luminosity of $42\,\mathrm{pb}^{-1}$, taken at the beginning of the 2015 pp run.

The top-antitop quark ($\mathrm{t\bar{t}}$) production cross section has been measured for the first time by the CMS in proton-proton collisions at $\sqrt{s} = 13\,\mathrm{TeV}$ [17]. The measurement is performed by analyzing events with one electron and one muon and at least two jets. The results are obtained through an event-counting analysis. The measured cross section is $\sigma_{\mathrm{t\bar{t}}} = 772 \pm 60(\mathrm{stat}) \pm 62(\mathrm{syst}) \pm 93(\mathrm{lumi})$ pb, resulting in a total relative uncertainty of 16.4% (Fig. 6). This measurement is consistent with the standard model prediction of $\sigma_{\mathrm{t\bar{t}}}^{\mathrm{NNLO+NNLL}} = 832^{+40}_{-46}$ pb for a top quark mass of 172.5 GeV, and also with a recent measurement from the ATLAS Collaboration [18].

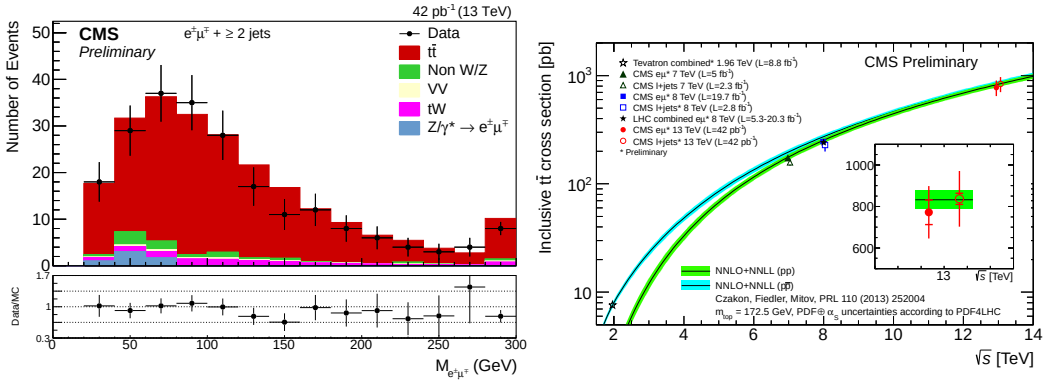

Figure 6. Left: Distribution of the dilepton invariant mass after all selections [17]. The last bin contains the overflow events. The ratios of data to the sum of the expected yields are given at the bottom. Right: Top quark pair production cross section in $p\bar{p}$ and pp collisions as a function of center-of-mass energy.

The total inclusive and the normalized differential cross sections for the production of top quark pairs have been determined in proton-proton collisions at 13 TeV [19, 20]. The measurements are performed in the l+jets decay channels with an electron or a muon in the final state. The $t\bar{t}$ production cross section is measured as a function of p_T and y of the top quarks and as a function of p_T, y, and invariant mass of the $t\bar{t}$ system, as well as of the jet multiplicity. Due to the limited available integrated luminosity the precision of the measurement is mostly dominated by the statistical uncertainties. However, in some kinematic regions the uncertainties in the parton shower and hadronization model are higher. The results are compared to several standard model calculations (Fig. 7-left). All calculations are compatible with the measured results though the POWHEG simulation shows the best agreement in the description of $p_T(t\bar{t})$. In the l+jets decay channels we measure a total inclusive $t\bar{t}$ production cross section of $836 \pm 27(\text{stat}) \pm 88(\text{syst}) \pm 100(\text{lumi})$ pb. This is in good agreement with the NNLO standard model prediction, hence no significant deviation from the standard model prediction is observed.

The measurement of single top production helps testing QCD and electroweak processes, specifically the tWb vertex, and the CKM matrix element V_{tb}. In the analysis, events with one muon (from $t \to W \to \mu$ or via $t \to W \to \tau \to \mu$ decays) in the final state are selected. The signal can be most easily got from a fit to the η distribution of the (light) recoil jet.

A measurement of the t-channel single top-quark cross section has been performed using the very first proton-proton collisions at 13 TeV [21]. Events are selected with one muon in the final state. The signal is extracted from a fit to the pseudorapidity distribution of the recoiling jet. The inclusive cross section is measured to be $\sigma_{\text{t-ch}} = 274 \pm 98(\text{stat}) \pm 52(\text{syst}) \pm 33(\text{lumi})$. The observed (expected) significance of the signal contribution is 3.5 (2.7) standard deviations with respect to the background-only hypothesis. The magnitude of the CKM matrix element V_{tb} is also calculated, yielding $|V_{tb}| = 1.12 \pm 0.24(\text{exp}) \pm 0.02(\text{theo})$. The results are found to be in agreement with predictions by the standard model (Fig 7-right).

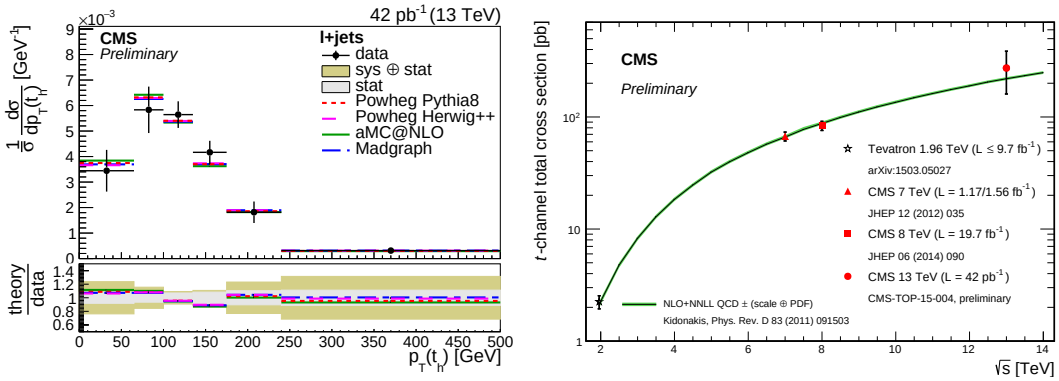

Figure 7. Left: Normalized differential cross sections as a function of p_T(t) compared to the predictions of several MC event generators [19]. Right: The t-channel single top-quark cross section summary of the most precise CMS measurements in comparison with QCD calculations [21].

4 Exotica

A search for narrow resonances decaying into a pair of jets has been performed using 42 pb^{-1} of pp collisions at $\sqrt{s}$ = 13 TeV. The dijet invariant mass distribution is measured to be a smoothly falling distribution (Fig. 8-left), as expected within the standard model. In the analyzed data sample there is no significant evidence for new particle production. We present generic upper limits that are applicable to any model of narrow dijet resonance production. A list specific lower limits is set on the mass of string resonances, excited quarks, axigluons, colorons, color octet scalars, and scalar diquarks (Fig. 8-right). These give the most stringent constraint to date on the mass of string resonances, a lower mass limit of 5.1 TeV. This dijet resonance search is more sensitive than the previous Run 1 searches for dijet resonances beyond 5 TeV.

Acknowledgments

The author wishes to thank to the Hungarian Scientific Research Fund (K 109703), and the Swiss National Science Foundation (SCOPES 152601) for their support.

References

[1] V. Khachatryan et al. (CMS), Phys. Lett. B **751**, 143 (2015), 1507.05915
[2] T. Sjöstrand, S. Mrenna, P. Skands, JHEP **05**, 026 (2006), hep-ph/0603175
[3] T. Sjöstrand, S. Mrenna, P.Z. Skands, Comput. Phys. Commun. **178**, 852 (2008), 0710.3820
[4] CMS Collaboration (2014), CMS-PAS-GEN-14-001
[5] K. Werner, F.M. Liu, T. Pierog, Phys. Rev. C **74**, 044902 (2006), hep-ph/0506232
[6] T. Pierog, I. Karpenko, J.M. Katzy, E. Yatsenko, K. Werner (2013), dESY-13-125, 1306.0121
[7] S. Agostinelli et al. (GEANT4), Nucl. Instrum. Meth. A **506**, 250 (2003)
[8] CMS Collaboration (2015), CMS-DP-2015-011

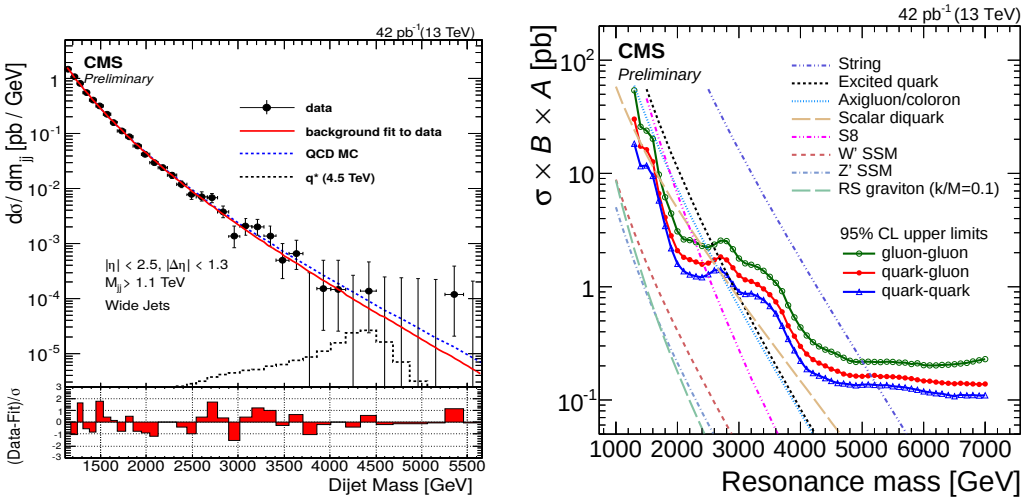

Figure 8. Left: Dijet mass spectrum from wide jets (points) compared to a smooth fit (solid) and to predictions including detector simulation of QCD (dashed) and an excited quark signal (histogram) [22]. The QCD prediction has been normalized to the data. Right: The observed 95% confidence level upper limits for dijet resonances of the type gluon-gluon, quark-gluon, and quark-quark, compared to theoretical predictions [22].

[9] A.M. Rossi, G. Vannini, A. Bussière, E. Albini, D. D'Alessandro, G. Giacomelli, Nucl. Phys. B **84**, 269 (1975)

[10] W. Thome et al. (Aachen-CERN-Heidelberg-Munich), Nucl. Phys. B **129**, 365 (1977)

[11] G.J. Alner et al. (UA5), Z. Phys. C **33**, 1 (1986)

[12] G.J. Alner et al. (UA5), Phys. Rept. **154**, 247 (1987)

[13] B.B. Back et al. (PHOBOS), Phys. Rev. Lett. **93**, 082301 (2004), nucl-ex/0311009

[14] K. Aamodt et al. (ALICE), Eur. Phys. J. C **68**, 89 (2010), 1004.3034

[15] V. Khachatryan et al. (CMS) (2015), 1510.03068

[16] K. Dusling, R. Venugopalan, Phys. Rev. D **87**, 094034 (2013), 1302.7018

[17] V. Khachatryan et al. (CMS) (2015), 1510.05302

[18] ATLAS Collaboration (2015), ATLAS-CONF-2015-033

[19] CMS Collaboration (2015), CMS-PAS-TOP-15-005

[20] CMS Collaboration (2015), CMS-PAS-TOP-15-010

[21] CMS Collaboration (2015), CMS-PAS-TOP-15-004

[22] CMS Collaboration (2015), CMS-PAS-EXO-15-001